

**What Photometric Images Have (and Haven't)**

**Taught us About TSI**

**Stephen Walton, San Fernando Observatory**

**Cal State Northridge**

**SORCE 2004  
October 28, 2004**

**What Photometric Images Have (and Haven't)**

**Taught us About TSI**

**Stephen Walton, San Fernando Observatory**

**Cal State Northridge**

**SORCE 2004  
October 28, 2004**

Colleagues

**What Photometric Images Have (and Haven't)**

**Taught us About TSI**

**Stephen Walton, San Fernando Observatory**

**Cal State Northridge**

**SORCE 2004  
October 28, 2004**

Colleagues

Gary Chapman

Angela Cookson

Jan Dobias

Dora Preminger

**What Photometric Images Have (and Haven't)**

**Taught us About TSI**

**Stephen Walton, San Fernando Observatory**

**Cal State Northridge**

**SORCE 2004  
October 28, 2004**

Colleagues

Gary Chapman

Angela Cookson

Jan Dobias

Dora Preminger

and students too numerous to mention...

# **What Photometric Images Have (and Haven't)**

## **Taught us About TSI**

**Stephen Walton, San Fernando Observatory**

**Cal State Northridge**

**SORCE 2004  
October 28, 2004**

Colleagues

Gary Chapman

Angela Cookson

Jan Dobias

Dora Preminger

and students too numerous to mention...

We also gratefully acknowledge the continuing support of CSUN, NASA, and NSF for the photometry program at SFO.

# Outline

## Outline

- Overview of the Problem

## Outline

- Overview of the Problem
- Our Data: SFO Photometric Images

## Outline

- Overview of the Problem
- Our Data: SFO Photometric Images
- Results

## Outline

- Overview of the Problem
- Our Data: SFO Photometric Images
- Results
  - Modeling TSI From Ground Based Photometric Images

## Outline

- Overview of the Problem
- Our Data: SFO Photometric Images
- Results
  - Modeling TSI From Ground Based Photometric Images
  - Photometry of Individual Solar Features

## Outline

- Overview of the Problem
- Our Data: SFO Photometric Images
- Results
  - Modeling TSI From Ground Based Photometric Images
  - Photometry of Individual Solar Features
  - Bolometric Image and “Image”

## Outline

- Overview of the Problem
- Our Data: SFO Photometric Images
- Results
  - Modeling TSI From Ground Based Photometric Images
  - Photometry of Individual Solar Features
  - Bolometric Image and “Image”
- Summary and Future Work

## Overview

*Goal:* Understand the sources of variability of the total solar irradiance  $S$  and its dependence on wavelength

## Overview

*Goal:* Understand the sources of variability of the total solar irradiance  $S$  and its dependence on wavelength

*A Partial List of Questions*

## Overview

*Goal:* Understand the sources of variability of the total solar irradiance  $S$  and its dependence on wavelength

### *A Partial List of Questions*

- What do we conclude about contributions to changes in  $S$  due to changes in the spectrum?

## Overview

*Goal:* Understand the sources of variability of the total solar irradiance  $S$  and its dependence on wavelength

### *A Partial List of Questions*

- What do we conclude about contributions to changes in  $S$  due to changes in the spectrum?
- What are the effects of various solar features on  $S$ ?

## Overview

*Goal:* Understand the sources of variability of the total solar irradiance  $S$  and its dependence on wavelength

### *A Partial List of Questions*

- What do we conclude about contributions to changes in  $S$  due to changes in the spectrum?
- What are the effects of various solar features on  $S$ ?
- What might we learn from newly available bolometric images?

# SFO Photometric Images

## SFO Photometric Images

- CFDT1: 5'' × 5'' pixels
  - Began operation in 1985
  - 672.3 nm, 10 nm bandpass (average level 0.98 continuum)
  - 393.4 nm, 1 nm bandpass added Spring 1988
  - 472.3 nm, 10 nm bandpass added Spring 1988

## SFO Photometric Images

- CFDT1:  $5'' \times 5''$  pixels
  - Began operation in 1985
  - 672.3 nm, 10 nm bandpass (average level 0.98 continuum)
  - 393.4 nm, 1 nm bandpass added Spring 1988
  - 472.3 nm, 10 nm bandpass added Spring 1988
- CFDT2:  $2.5'' \times 2.5''$  pixels
  - Began operation in 1992
  - Same three bandpasses as CFDT1 plus

## SFO Photometric Images

- CFDT1:  $5'' \times 5''$  pixels
  - Began operation in 1985
  - 672.3 nm, 10 nm bandpass (average level 0.98 continuum)
  - 393.4 nm, 1 nm bandpass added Spring 1988
  - 472.3 nm, 10 nm bandpass added Spring 1988
- CFDT2:  $2.5'' \times 2.5''$  pixels
  - Began operation in 1992
  - Same three bandpasses as CFDT1 plus
  - 393.4 nm, 0.3 nm bandpass
  - 997.0 nm, 10 nm bandpass
  - 780.0 nm, 10 nm bandpass added 2003

# Definitions

## Definitions

- $S$ : the total solar irradiance as a function of time

## Definitions

- $S$ : the total solar irradiance as a function of time
- $I(x, y)$ : intensity of solar disk at  $x, y$

## Definitions

- $S$ : the total solar irradiance as a function of time
- $I(x, y)$ : intensity of solar disk at  $x, y$
- $I_q(\mu)$ : quiet sun limb darkening curve in same units as  $I(x, y)$

## Definitions

- $S$ : the total solar irradiance as a function of time
- $I(x, y)$ : intensity of solar disk at  $x, y$
- $I_q(\mu)$ : quiet sun limb darkening curve in same units as  $I(x, y)$
- Contrast  $C(x, y) \equiv \frac{I(x, y)}{I_q(\mu)} - 1$

# Modeling $S$

## Modeling $S$

- A generic photometric quantity  $X$  can be computed by

$$X = \sum_{\text{feature pixels}} A_i C_i \phi(\mu_i)$$

## Modeling $S$

- A generic photometric quantity  $X$  can be computed by

$$X = \sum_{\text{feature pixels}} A_i C_i \phi(\mu_i)$$

- $A_i$ : area of the  $i$ 'th feature pixel, in fractions of the solar disk
- $C_i$ : measured contrast of the  $i$ th feature pixel
- $\mu_i$ :  $\cos \theta$  of the  $i$ 'th pixel,  $\theta$  the heliocentric angle
- $\phi(\mu)$ : limb darkening curve normalized to unit integral over disk

## Modeling $S$

- A generic photometric quantity  $X$  can be computed by

$$X = \sum_{\text{feature pixels}} A_i C_i \phi(\mu_i)$$

- $A_i$ : area of the  $i$ 'th feature pixel, in fractions of the solar disk
  - $C_i$ : measured contrast of the  $i$ th feature pixel
  - $\mu_i$ :  $\cos \theta$  of the  $i$ 'th pixel,  $\theta$  the heliocentric angle
  - $\phi(\mu)$ : limb darkening curve normalized to unit integral over disk
- SFO computes the following:

## Modeling $S$

- A generic photometric quantity  $X$  can be computed by

$$X = \sum_{\text{feature pixels}} A_i C_i \phi(\mu_i)$$

- $A_i$ : area of the  $i$ 'th feature pixel, in fractions of the solar disk
  - $C_i$ : measured contrast of the  $i$ th feature pixel
  - $\mu_i$ :  $\cos \theta$  of the  $i$ 'th pixel,  $\theta$  the heliocentric angle
  - $\phi(\mu)$ : limb darkening curve normalized to unit integral over disk
- SFO computes the following:
    - $D_r$  = red deficit (sum over red sunspot pixels)

## Modeling $S$

- A generic photometric quantity  $X$  can be computed by

$$X = \sum_{\text{feature pixels}} A_i C_i \phi(\mu_i)$$

- $A_i$ : area of the  $i$ 'th feature pixel, in fractions of the solar disk
  - $C_i$ : measured contrast of the  $i$ th feature pixel
  - $\mu_i$ :  $\cos \theta$  of the  $i$ 'th pixel,  $\theta$  the heliocentric angle
  - $\phi(\mu)$ : limb darkening curve normalized to unit integral over disk
- SFO computes the following:
    - $D_r$  = red deficit (sum over red sunspot pixels)
    - $E_r$  = red excess (red facular pixels)

## Modeling $S$

- A generic photometric quantity  $X$  can be computed by

$$X = \sum_{\text{feature pixels}} A_i C_i \phi(\mu_i)$$

- $A_i$ : area of the  $i$ 'th feature pixel, in fractions of the solar disk
  - $C_i$ : measured contrast of the  $i$ th feature pixel
  - $\mu_i$ :  $\cos \theta$  of the  $i$ 'th pixel,  $\theta$  the heliocentric angle
  - $\phi(\mu)$ : limb darkening curve normalized to unit integral over disk
- SFO computes the following:
    - $D_r$  = red deficit (sum over red sunspot pixels)
    - $E_r$  = red excess (red facular pixels)
    - $\Sigma_r$  = red photometric sum (*all* pixels on the red images)

## Modeling $S$

- A generic photometric quantity  $X$  can be computed by

$$X = \sum_{\text{feature pixels}} A_i C_i \phi(\mu_i)$$

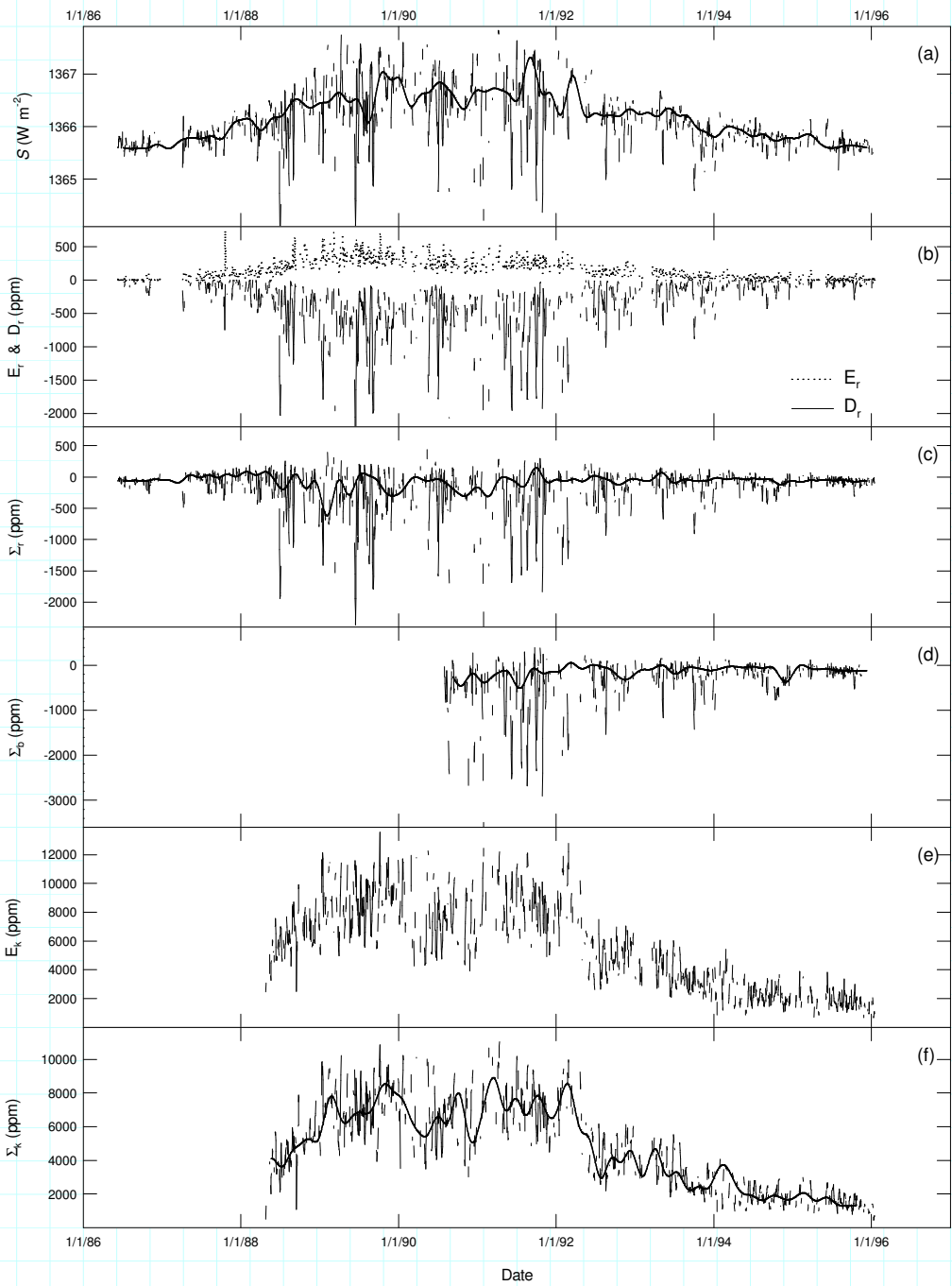
- $A_i$ : area of the  $i$ 'th feature pixel, in fractions of the solar disk
  - $C_i$ : measured contrast of the  $i$ th feature pixel
  - $\mu_i$ :  $\cos \theta$  of the  $i$ 'th pixel,  $\theta$  the heliocentric angle
  - $\phi(\mu)$ : limb darkening curve normalized to unit integral over disk
- SFO computes the following:
    - $D_r$  = red deficit (sum over red sunspot pixels)
    - $E_r$  = red excess (red facular pixels)
    - $\Sigma_r$  = red photometric sum (*all* pixels on the red images)
    - $D_K$ ,  $E_K$ , and  $\Sigma_K$  computed similarly from Ca II K images.

## Modeling $S$

- A generic photometric quantity  $X$  can be computed by

$$X = \sum_{\text{feature pixels}} A_i C_i \phi(\mu_i)$$

- $A_i$ : area of the  $i$ 'th feature pixel, in fractions of the solar disk
  - $C_i$ : measured contrast of the  $i$ th feature pixel
  - $\mu_i$ :  $\cos \theta$  of the  $i$ 'th pixel,  $\theta$  the heliocentric angle
  - $\phi(\mu)$ : limb darkening curve normalized to unit integral over disk
- SFO computes the following:
    - $D_r$  = red deficit (sum over red sunspot pixels)
    - $E_r$  = red excess (red facular pixels)
    - $\Sigma_r$  = red photometric sum (*all* pixels on the red images)
    - $D_K$ ,  $E_K$ , and  $\Sigma_K$  computed similarly from Ca II K images.
  - $S$  modeled using linear regressions of various combinations of these indices.



# Implications

## Implications

Preminger, Walton, & Chapman 2002, *JGR* **107**, SH6-1

## Implications

Preminger, Walton, & Chapman 2002, *JGR* **107**, SH6-1

- $\Sigma_r$  vs. time for cycle 22 is virtually flat  $\Rightarrow$  continuum variations make no contribution to the 11-year variation in  $S$ , although they are highly significant on active region timescales

## Implications

Preminger, Walton, & Chapman 2002, *JGR* **107**, SH6-1

- $\Sigma_r$  vs. time for cycle 22 is virtually flat  $\Rightarrow$  continuum variations make no contribution to the 11-year variation in  $S$ , although they are highly significant on active region timescales
- $\Sigma_K$  is strongly correlated with 11-year variation  $\Rightarrow$  line blanketing changes drive the 11-year change in  $S$

## Implications

Preminger, Walton, & Chapman 2002, *JGR* **107**, SH6-1

- $\Sigma_r$  vs. time for cycle 22 is virtually flat  $\Rightarrow$  continuum variations make no contribution to the 11-year variation in  $S$ , although they are highly significant on active region timescales
- $\Sigma_K$  is strongly correlated with 11-year variation  $\Rightarrow$  line blanketing changes drive the 11-year change in  $S$
- In this view, we divide influences on  $S$  by spectrum rather than feature type

## Implications

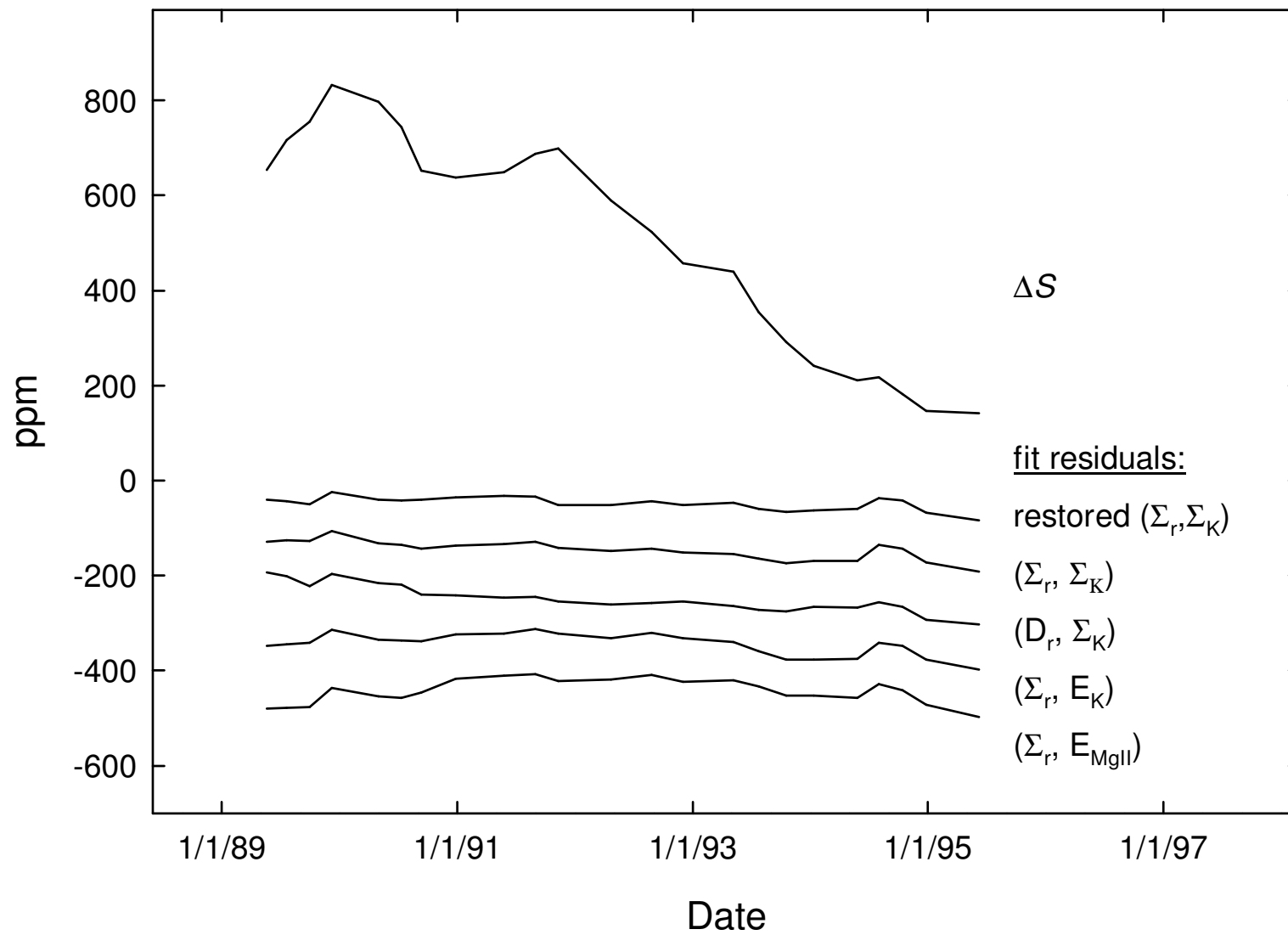
Preminger, Walton, & Chapman 2002, *JGR* **107**, SH6-1

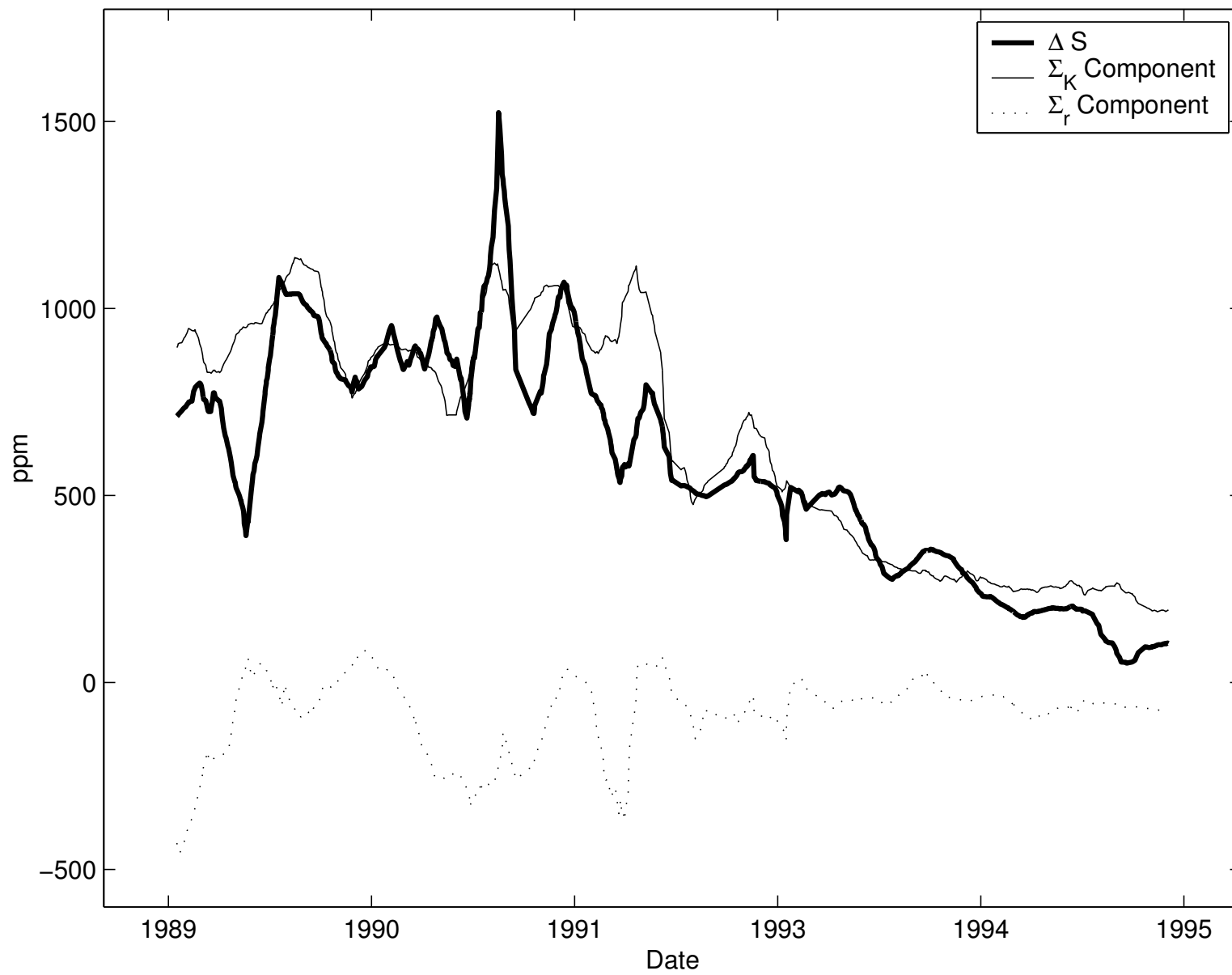
- $\Sigma_r$  vs. time for cycle 22 is virtually flat  $\Rightarrow$  continuum variations make no contribution to the 11-year variation in  $S$ , although they are highly significant on active region timescales
- $\Sigma_K$  is strongly correlated with 11-year variation  $\Rightarrow$  line blanketing changes drive the 11-year change in  $S$
- In this view, we divide influences on  $S$  by spectrum rather than feature type
- For quantitative analysis, we use a model of the form  $S = S_0 + a\Sigma_r + b\Sigma_K$ .

## Implications

Preminger, Walton, & Chapman 2002, *JGR* **107**, SH6-1

- $\Sigma_r$  vs. time for cycle 22 is virtually flat  $\Rightarrow$  continuum variations make no contribution to the 11-year variation in  $S$ , although they are highly significant on active region timescales
- $\Sigma_K$  is strongly correlated with 11-year variation  $\Rightarrow$  line blanketing changes drive the 11-year change in  $S$
- In this view, we divide influences on  $S$  by spectrum rather than feature type
- For quantitative analysis, we use a model of the form  $S = S_0 + a\Sigma_r + b\Sigma_K$ . This matches observed composite  $S$  for all of cycle 22 (June 1988–Sept 1996) with  $R = 0.96$  and  $\sigma = 0.18 \text{ W m}^{-2}$  (130 ppm).





## Conclusions on Models of $S$

## Conclusions on Models of $S$

- The main source of variability on rotational timescales is sunspot deficit, on solar cycle timescales facular excess.

## Conclusions on Models of $S$

- The main source of variability on rotational timescales is sunspot deficit, on solar cycle timescales facular excess. Solar features are cause of most of TSI variation

## Conclusions on Models of $S$

- The main source of variability on rotational timescales is sunspot deficit, on solar cycle timescales facular excess. Solar features are cause of most of TSI variation
- Solar cycle variations in  $S$  are dominated by changes in line blanketing:

## Conclusions on Models of $S$

- The main source of variability on rotational timescales is sunspot deficit, on solar cycle timescales facular excess. Solar features are cause of most of TSI variation
- Solar cycle variations in  $S$  are dominated by changes in line blanketing: not really a surprise when comparing the vertical temperature stratification of faculae and the quiet sun.

## Conclusions on Models of $S$

- The main source of variability on rotational timescales is sunspot deficit, on solar cycle timescales facular excess. Solar features are cause of most of TSI variation
- Solar cycle variations in  $S$  are dominated by changes in line blanketing: not really a surprise when comparing the vertical temperature stratification of faculae and the quiet sun.
- When SIM data become available, they should show that the 11-year variation in  $S$  will be primarily due to changes in the depths of spectral lines

## Conclusions on Models of $S$

- The main source of variability on rotational timescales is sunspot deficit, on solar cycle timescales facular excess. Solar features are cause of most of TSI variation
- Solar cycle variations in  $S$  are dominated by changes in line blanketing: not really a surprise when comparing the vertical temperature stratification of faculae and the quiet sun.
- When SIM data become available, they should show that the 11-year variation in  $S$  will be primarily due to changes in the depths of spectral lines  $\Rightarrow$  they will mainly occur shortward of 400 nm.
- Extrapolation of model to  $\Sigma_K = 0$  yields a TSI about  $0.3 \text{ W/m}^2$  below current solar minimum values

## Conclusions on Models of $S$

- The main source of variability on rotational timescales is sunspot deficit, on solar cycle timescales facular excess. Solar features are cause of most of TSI variation
- Solar cycle variations in  $S$  are dominated by changes in line blanketing: not really a surprise when comparing the vertical temperature stratification of faculae and the quiet sun.
- When SIM data become available, they should show that the 11-year variation in  $S$  will be primarily due to changes in the depths of spectral lines  $\Rightarrow$  they will mainly occur shortward of 400 nm.
- Extrapolation of model to  $\Sigma_K = 0$  yields a TSI about  $0.3 \text{ W/m}^2$  below current solar minimum values
- Modeling effects on climate due to UV variations are important, because the rest of the spectrum likely does not vary much.

## Feature Contributions to $S$

## Feature Contributions to $S$

Walton, Preminger, and Chapman 2003, *Ap.J.* **590**, 1088

## Feature Contributions to $S$

Walton, Preminger, and Chapman 2003, *Ap.J.* **590**, 1088

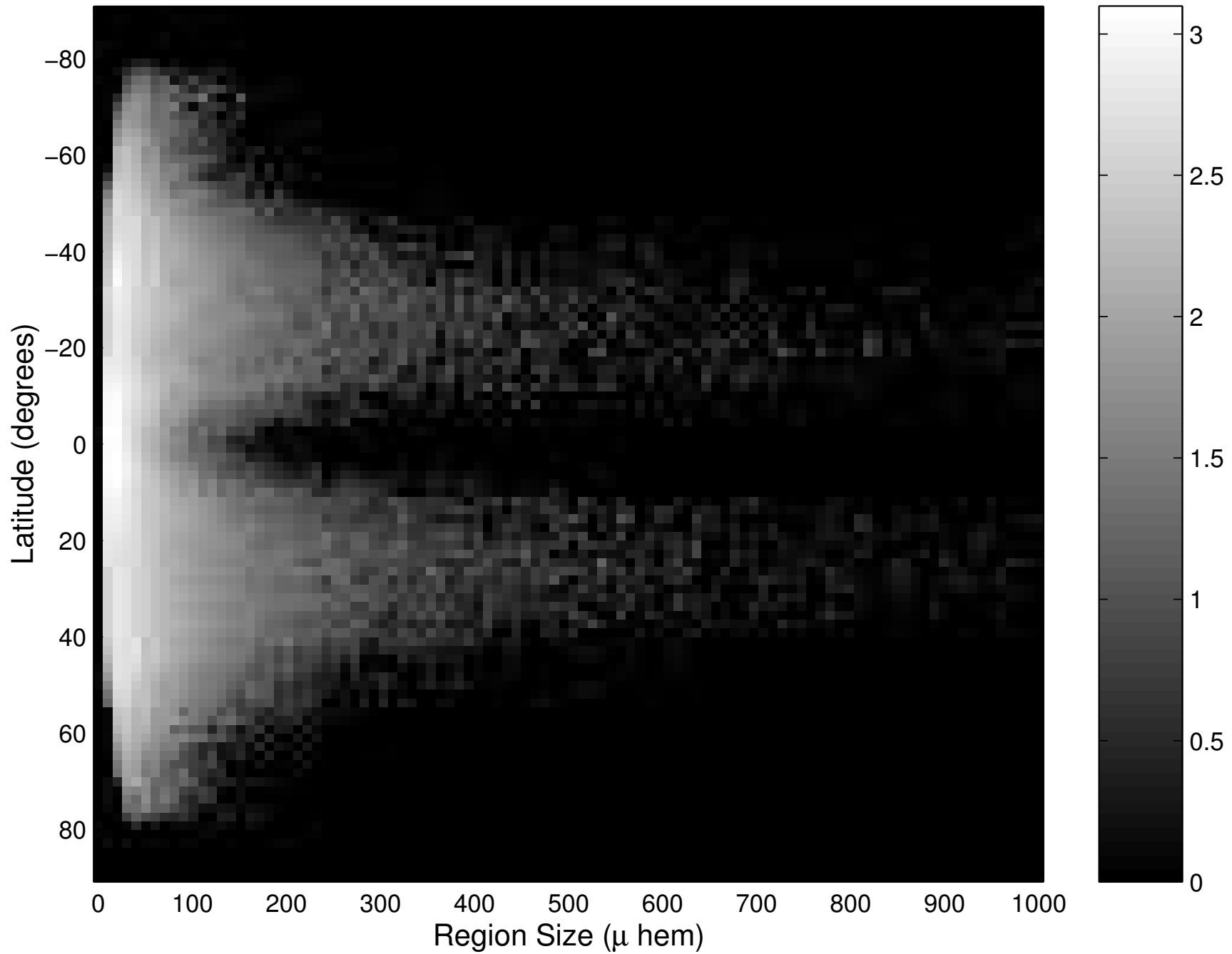
- The eleven year variation in  $\Sigma_K$  is dominated by changes in the excess  $E_K$

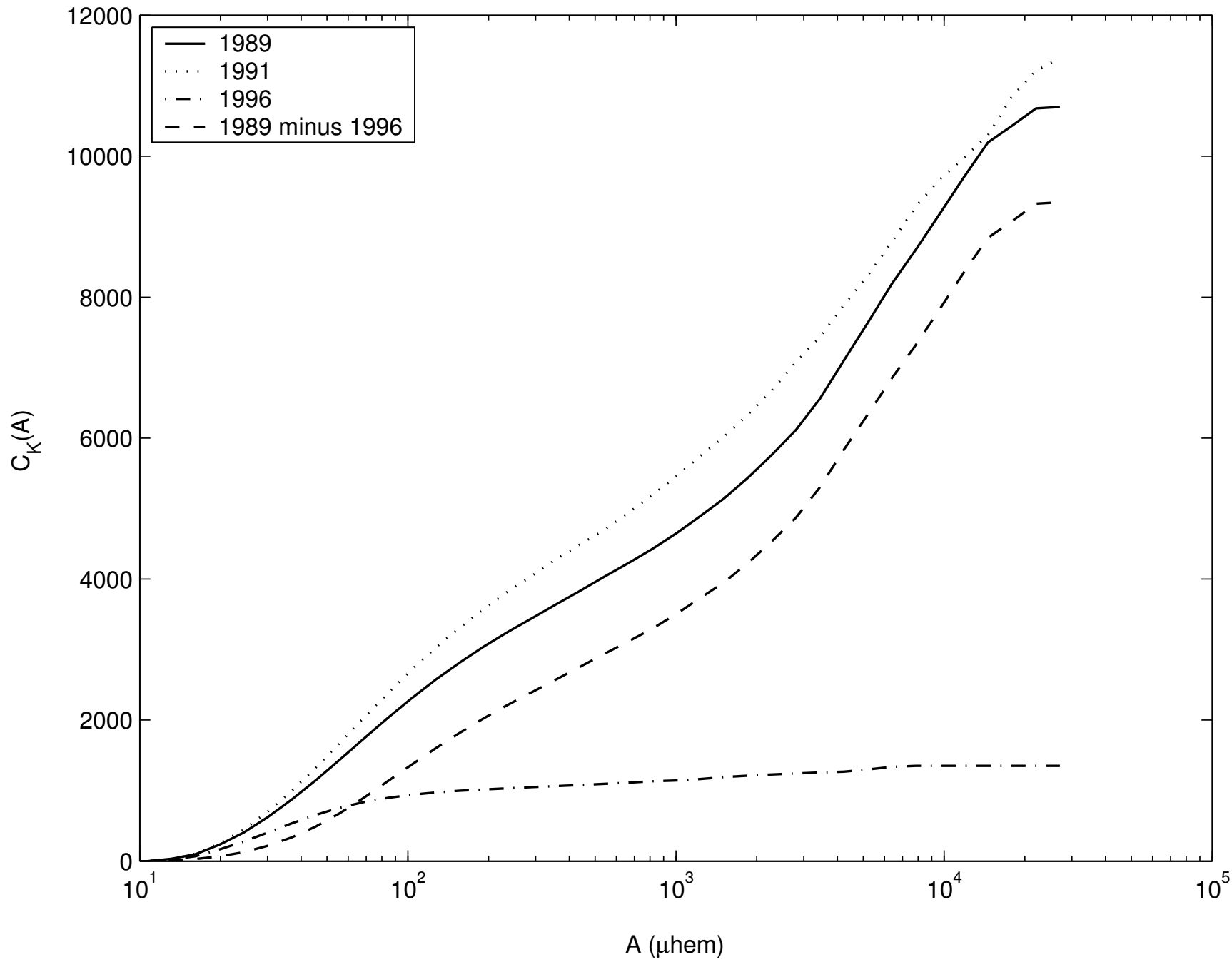
## Feature Contributions to $S$

Walton, Preminger, and Chapman 2003, *Ap.J.* **590**, 1088

- The eleven year variation in  $\Sigma_K$  is dominated by changes in the excess  $E_K$
- Thus, photometry of individual bright K features should tell us the relative contribution of each feature to the 11-year variability in  $S$

Latitude Distribution of Faculae with Area, 1989





## Conclusions on Relative Contributions of Features to $S$

## Conclusions on Relative Contributions of Features to $S$

- Large features produce most of the change in  $E_K$ , and by extension  $S$ , from solar maximum to solar minimum.

## Conclusions on Relative Contributions of Features to $S$

- Large features produce most of the change in  $E_K$ , and by extension  $S$ , from solar maximum to solar minimum.
- Computations show roughly 80% of the solar cycle change in  $S$  is due to features larger than 100 millionths of the solar hemisphere.

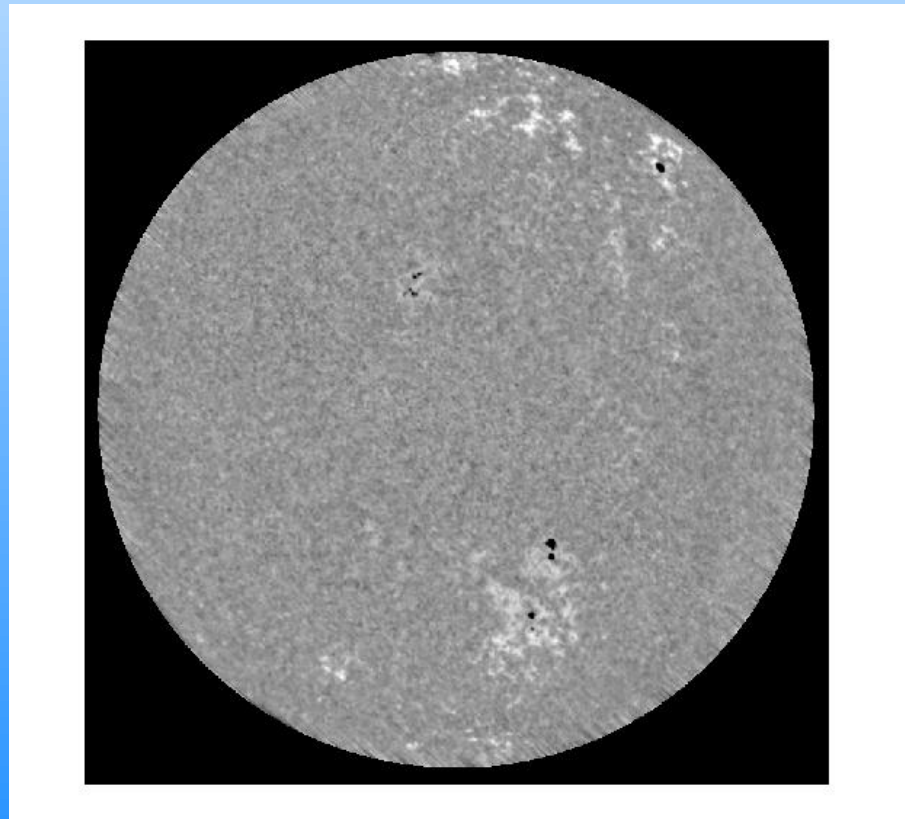
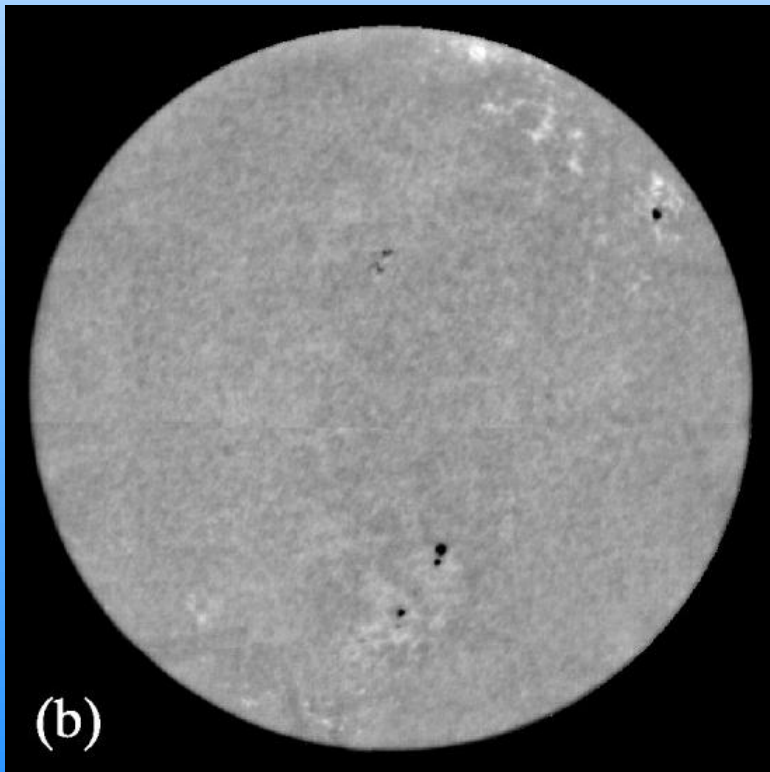
## Conclusions on Relative Contributions of Features to $S$

- Large features produce most of the change in  $E_K$ , and by extension  $S$ , from solar maximum to solar minimum.
- Computations show roughly 80% of the solar cycle change in  $S$  is due to features larger than 100 millionths of the solar hemisphere.
- Direct measurements of  $D_r$  and  $E_K$  are less likely to be misleading than assumptions about the contrasts of solar features.

And now...

And now...

SBI Bolometric and SFO "Bolometric" Images for 1 September 2003



# Data Availability

## **Data Availability**

The SFO Web site is <http://www.csun.edu/sfo>. Daily CFDT1 images are available for download; our photometric indices will appear there soon.

## Reconstruction of $S$ From Sunspots Only

## Reconstruction of $S$ From Sunspots Only

- Despite importance of actual photometry, it is simply not available before 1986

## Reconstruction of $S$ From Sunspots Only

- Despite importance of actual photometry, it is simply not available before 1986
- We need some other way to get to  $S$  on longer timescales

## Reconstruction of $S$ From Sunspots Only

- Despite importance of actual photometry, it is simply not available before 1986
- We need some other way to get to  $S$  on longer timescales
- Daily values of RGO areas not well correlated with TSI; graph of area vs. TSI shows definite curvature (Solanki and Fligge, etc.)

## Reconstruction of $S$ From Sunspots Only

- Despite importance of actual photometry, it is simply not available before 1986
- We need some other way to get to  $S$  on longer timescales
- Daily values of RGO areas not well correlated with TSI; graph of area vs. TSI shows definite curvature (Solanki and Fligge, etc.)
- Convolution of RGO areas with a finite impulse response (FIR) function produces an accurate TSI model

## Reconstruction of $S$ From Sunspots Only

- Despite importance of actual photometry, it is simply not available before 1986
- We need some other way to get to  $S$  on longer timescales
- Daily values of RGO areas not well correlated with TSI; graph of area vs. TSI shows definite curvature (Solanki and Fligge, etc.)
- Convolution of RGO areas with a finite impulse response (FIR) function produces an accurate TSI model
- This FIR shows TSI influences extend both ways in time from spot emergence.
- 
- See poster by Dora Preminger, this meeting.

## **A Few Comments on Solar Features**

## A Few Comments on Solar Features

Walton, Preminger, & Chapman 2003, *Solar Phys.* **213**, 301–317

## A Few Comments on Solar Features

Walton, Preminger, & Chapman 2003, *Solar Phys.* **213**, 301–317

- Identify bright and dark features using the *three-trigger* algorithm (Preminger, Walton, & Chapman 2001).

## A Few Comments on Solar Features

Walton, Preminger, & Chapman 2003, *Solar Phys.* **213**, 301–317

- Identify bright and dark features using the *three-trigger* algorithm (Preminger, Walton, & Chapman 2001).
- Allows direct identification of continuum faculae on red images

## A Few Comments on Solar Features

Walton, Preminger, & Chapman 2003, *Solar Phys.* **213**, 301–317

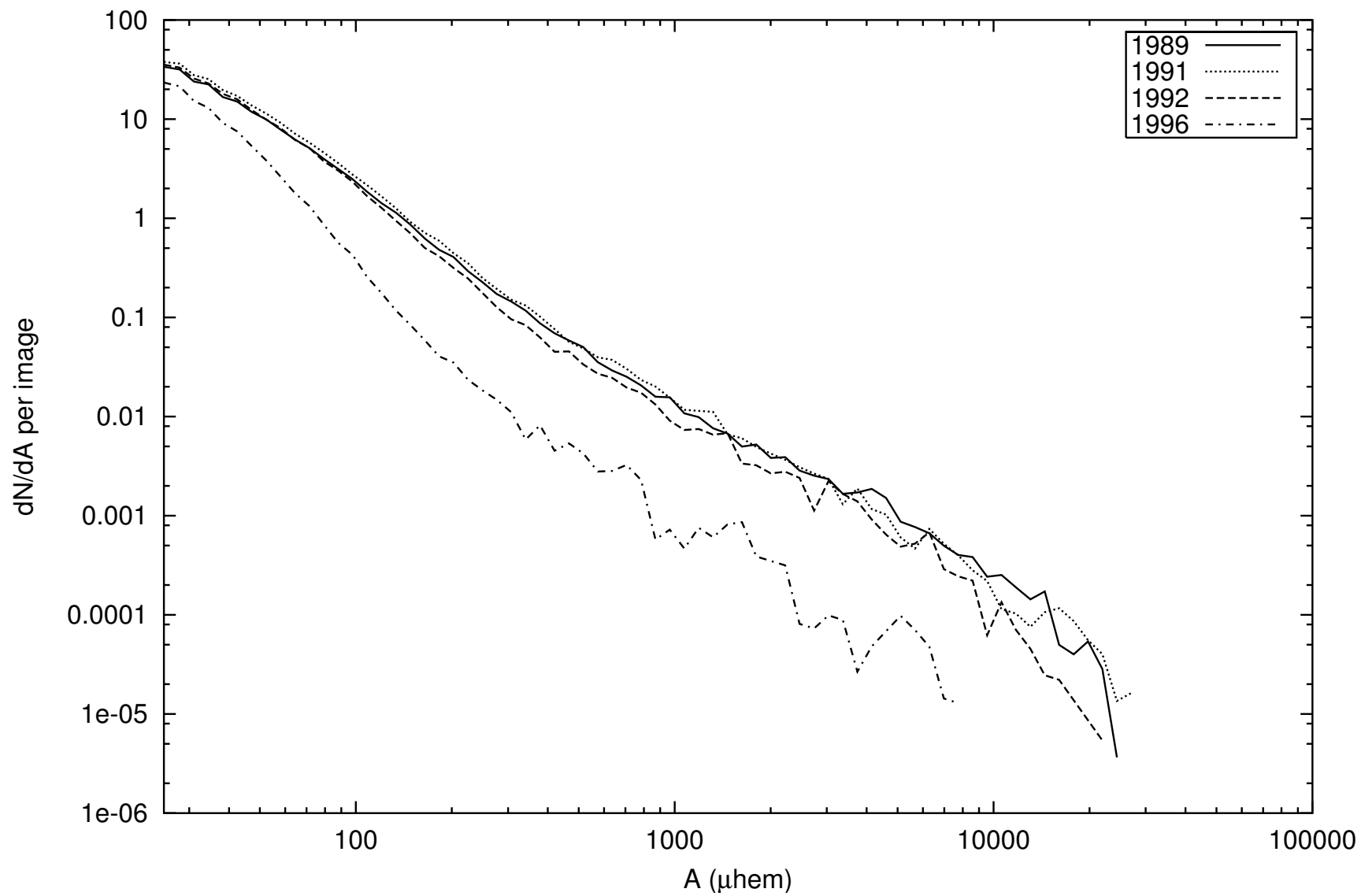
- Identify bright and dark features using the *three-trigger* algorithm (Preminger, Walton, & Chapman 2001).
- Allows direct identification of continuum faculae on red images
- Also examined pixels on red images which were co-spatial with Ca II K facular pixels

## A Few Comments on Solar Features

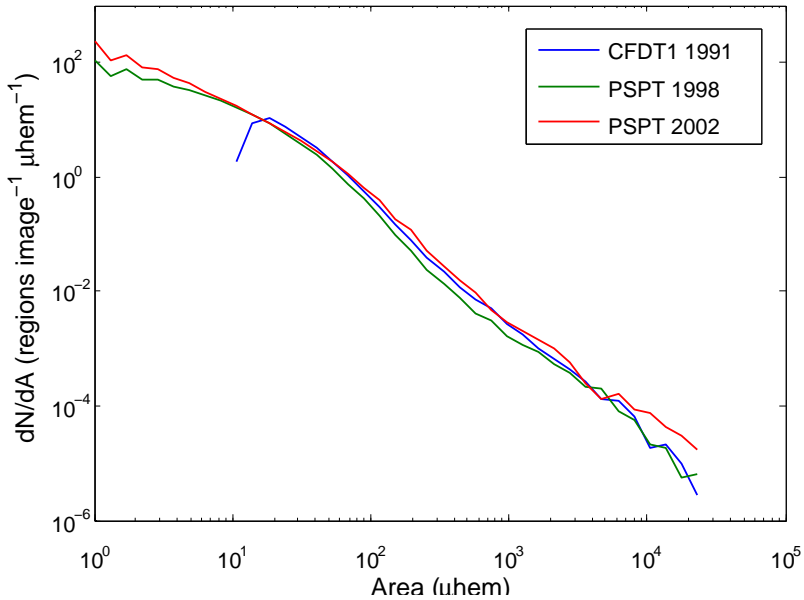
Walton, Preminger, & Chapman 2003, *Solar Phys.* **213**, 301–317

- Identify bright and dark features using the *three-trigger* algorithm (Preminger, Walton, & Chapman 2001).
- Allows direct identification of continuum faculae on red images
- Also examined pixels on red images which were co-spatial with Ca II K facular pixels
- A total of 18 000 sunspots, 147 000 continuum faculae, and 850 000 K faculae studied

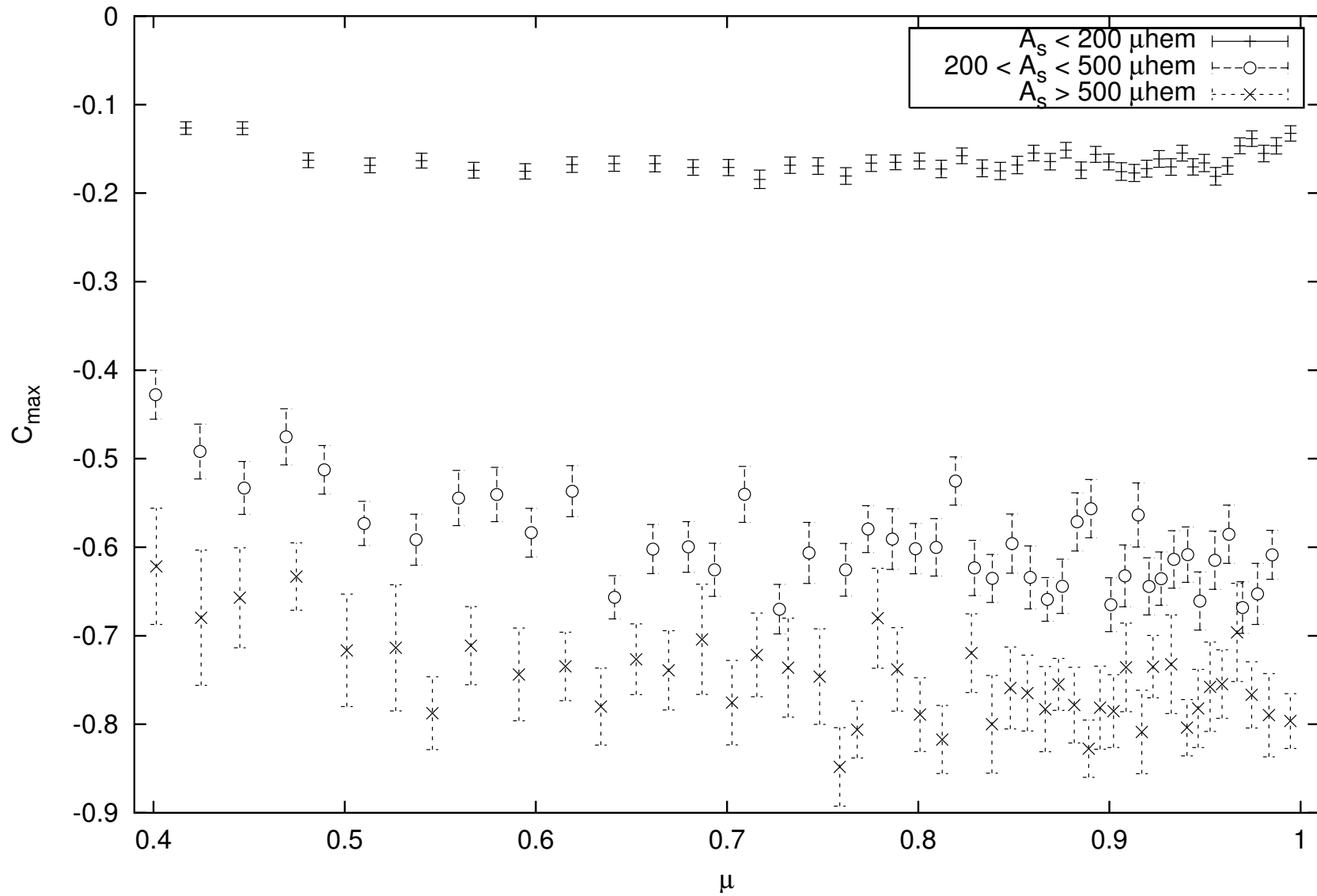
dN/dA for K Faculae



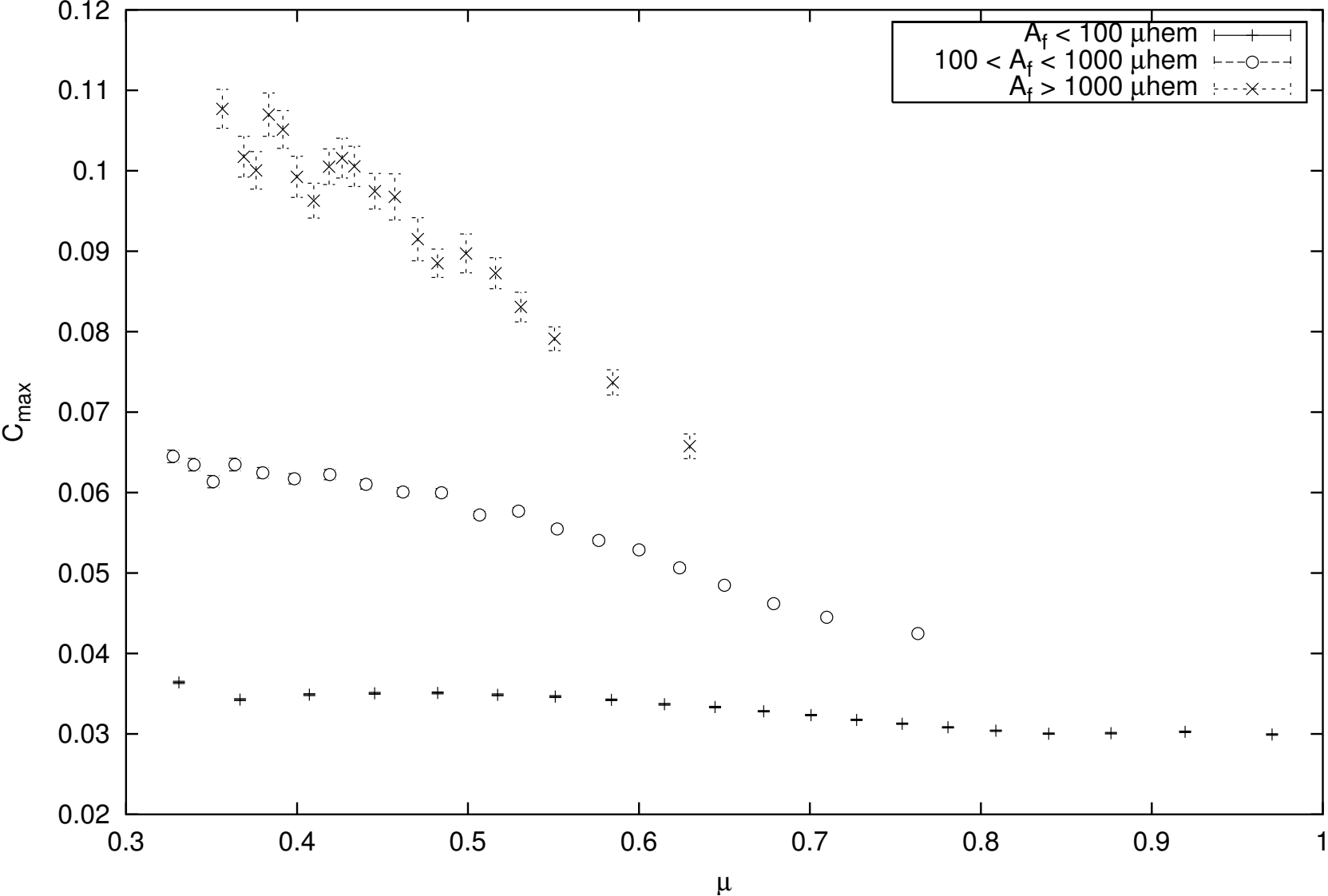
Area Distribution of PSPT K Faculae



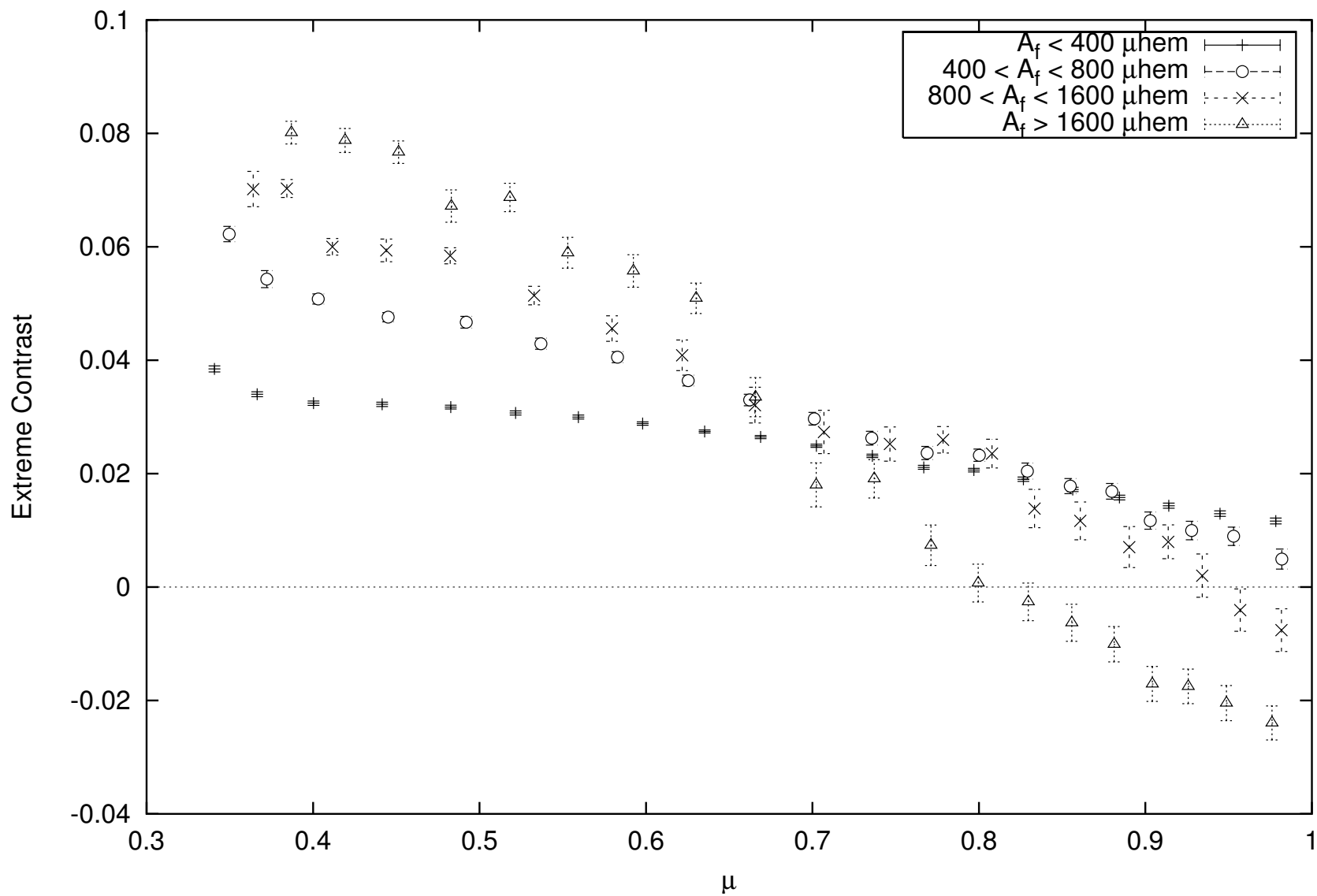
Binned Maximum Sunspot Contrast



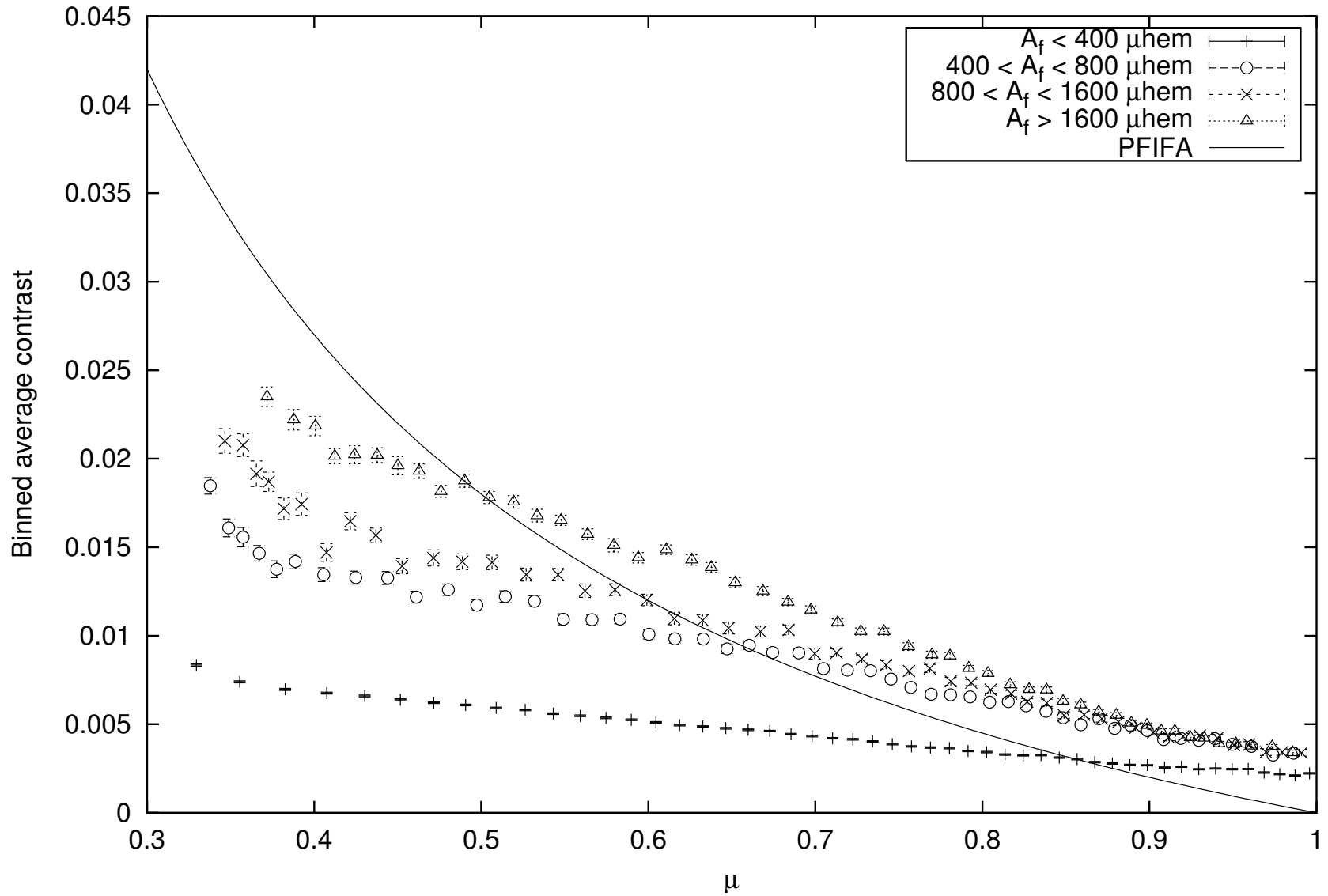
Maximum Red Facular Contrast



Red regions corresponding to K faculae



Red regions corresponding to K faculae



## **“Carry-Away” Conclusions for TSI Modeling**

## **“Carry-Away” Conclusions for TSI Modeling**

1. All faculae and sunspots are not created equal

## “Carry-Away” Conclusions for TSI Modeling

1. All faculae and sunspots are not created equal
2. We suggest, following Steinegger *et al.* among others, that (at minimum) area-dependent sunspot & facular contrasts should be used for TSI modeling
3. While some features which are bright in K are dark in continuum, on average bright in K  $\Rightarrow$  bright in continuum